Chk1 Suppresses a Caspase-2 Apoptotic Response to DNA Damage that Bypasses p53, Bcl-2, and Caspase-3

Samuel Sidi[1], **Takaomi Sanda**[1], **Richard D. Kennedy**[2], **Andreas T. Hagen**[1], **Cicely A. Jette**[1], **Raymond Hoffmans**[1], **Jennifer Pascual**[1], **Shintaro Imamura**[4], **Shuji Kishi**[4], **James F. Amatruda**[5], **John P. Kanki**[1], **Douglas R. Green**[6], **Alan A. D'Andrea**[2], and **A. Thomas Look**[1,3,*]

[1]Department of Pediatric Oncology

[2]Division of Genomic Stability and DNA Repair, Department of Radiation Oncology, Dana-Farber Cancer Institute, Harvard Medical School, Boston, MA 02115, USA

[3]Division of Hematology/Oncology, Department of Pediatrics, Children's Hospital Boston, Harvard Medical School, Boston, MA 02115, USA

[4]Department of Ophthalmology, Schepens Eye Research Institute, Harvard Medical School, Boston, MA 02114, USA

[5]Department of Pediatrics, Molecular Biology and Internal Medicine, University of Texas Southwestern Medical Center, Dallas, TX 75390, USA

[6]Department of Immunology, St. Jude Children's Research Hospital, Memphis, TN 38105, USA

SUMMARY

Evasion of DNA damage-induced cell death, via mutation of the *p53* tumor suppressor or overexpression of prosurvival Bcl-2 family proteins, is a key step toward malignant transformation and therapeutic resistance. We report that depletion or acute inhibition of checkpoint kinase 1 (Chk1) is sufficient to restore γ-radiation-induced apoptosis in *p53* mutant zebrafish embryos. Surprisingly, caspase-3 is not activated prior to DNA fragmentation, in contrast to classical intrinsic or extrinsic apoptosis. Rather, an alternative apoptotic program is engaged that cell autonomously requires *atm* (ataxia telangiectasia mutated), *atr* (ATM and Rad3-related) and *caspase-2*, and is not affected by *p53* loss or overexpression of *bcl-2/xl*. Similarly, Chk1 inhibitor-treated human tumor cells hyperactivate ATM, ATR, and caspase-2 after γ-radiation and trigger a caspase-2-dependent apoptotic program that bypasses p53 deficiency and excess Bcl-2. The evolutionarily conserved "Chk1-suppressed" pathway defines a novel apoptotic process, whose responsiveness to Chk1 inhibitors and insensitivity to *p53* and *BCL2* alterations have important implications for cancer therapy.

INTRODUCTION

The stress-inducible p53 protein acts as a central signal transduction node in the apoptotic response to DNA damage, mainly through its ability to transactivate intrinsic (mitochondrial) and extrinsic (death-receptor) pathway genes (Vousden and Lu, 2002). However, ample evidence supports the existence of p53-independent apoptotic responses to DNA damage. In *Drosophila* and mouse *p53* null embryos, for example, several cell types undergo apoptosis in

*Correspondence: E-mail: thomas_look@dfci.harvard.edu .

response to irradiation (IR), but with slower kinetics than $p53^{+/+}$ cells (Frenkel et al., 1999; Wichmann et al., 2006).

Candidate p53-independent apoptotic pathways have surfaced from in vitro studies. ATM/ATR-activated ABL, Chk1, and Chk2 can upregulate p73 protein levels in genotoxically challenged p53-deficient cells, restoring transactivation of *PUMA* and other proapoptotic p53 targets (Gong et al., 1999; Roos and Kaina, 2006; Urist et al., 2004; Yuan et al., 1999). p53-independent coupling of DNA damage to mitochondria can also occur through translocation of the nuclear orphan protein Nur77 into the cytosol, activation of nuclear and/or cytosolic caspase-2, or de novo ceramide synthesis by mitochondrial ceramide synthase, all converging on caspase-3 activation (Kolesnick and Fuks, 2003; Li et al., 2000; Lin et al., 2004; Zhivotovsky and Orrenius, 2005). Other p53-independent processes, involving MAPKs (e.g., SAPK/JNKs, p38) and the transcription factors E2F1, NF-κB, and FOXO1 couple DNA damage to caspase-3 activation by upregulating extrinsic pathway genes including *CASP8*, whose product activates caspase-3 in a mitochondria-dependent (Bcl-2-inhibitable) or -independent manner (Afshar et al., 2006; Huang et al., 2006; Kasibhatla et al., 1998; Yount et al., 2001). Whether the p53-independent pathways identified in vitro operate in vivo remains an active field of investigation.

Radio/chemoresistant *p53* mutant human cancer cell lines can be induced to die after genotoxic stress by pharmacologic or RNAi targeting of DNA damage-response (DDR) kinases involved in intra-S and/or G2/M checkpoint control, including ATM, ATR, Chk1, Chk2, Polo-like kinases (Plks) (reviewed in Castedo et al., 2004a), and most recently, the p38/MAPK-activated kinase MAPKAPK2 (MK-2) (Reinhardt et al., 2007). Such treatments might spare cells endowed with wild-type p53, presumably because their intact G1 checkpoint enables them to repair and thus survive DNA damage (Zhou and Bartek, 2004). Although the sensitization of —and selectivity for—*p53* mutant cells is at the root of anticancer strategies that target DDR kinases, none of these concepts have been rigorously tested in an animal model, and the underlying cell death mechanism is unclear.

To accelerate the discovery of physiologic p53-independent DDRs, we generated *p53* mutant zebrafish lines for use in whole organism-based modifier genetic screens (Berghmans et al., 2005). Zebrafish faithfully recapitulate mammalian intrinsic and extrinsic apoptotic signaling (reviewed in Pyati et al., 2007). The zebrafish $p53^{M214K}$ allele (or $p53^{e7}$, for mutation in exon 7) affects a conserved amino acid residue within a region of the DNA-binding domain corresponding to a mutational hotspot in human cancer, producing a transactivation-dead p53 variant. Homozygosity for $p53^{e7}$ recapitulates key traits associated with p53 deficiency in mammalian systems, including a strong tumor-prone phenotype, lack of G1-checkpoint function, and widespread cellular radioresistance (Berghmans et al., 2005).

Here we identify *chk1* as a gene whose loss restores IR-induced apoptosis in live *p53* mutant zebrafish embryos, and then use in vivo epistasis analyses to dissect the underlying mechanism. Unlike previously identified p53-independent apoptotic pathways, which restore caspase-3 activation downstream of defective p53, Chk1 depletion activates an ATM/ATR-caspase-2 axis that bypasses the mitochondrial and death-receptor pathways. We show that this "Chk1-suppressed" pathway can be triggered in p53-deficient or *BCL2*-overexpressing human tumor cells, providing a mechanistic rationale for the use of Chk1 inhibitors in cancer therapy.

RESULTS

A Morpholino Screen for Suppressors of $p53^{e7/e7}$ Radioresistance Identifies *chk1*

$p53^{e7/e7}$ mutant zebrafish embryos are refractory to DNA damage-induced cell death, as demonstrated by a nearly complete lack of acridine orange (AO) labeling in the brain and spinal chord of live embryos examined 7.5 hr after whole-body IR delivered at 18 hr postfertilization

(hpf) (Figure 1A and Figure 2A). We used morpholino antisense oligonucleotides (MOs) to knock down eight zebrafish S- and G2-checkpoint kinases and two nonkinase checkpoint regulators ($p21^{waf1/cip1}$ and $smc1$) in $p53^{e7/e7}$ mutant embryos. We assessed the ability of each knockdown to restore cell death (AO reactivity) at 7.5 hr post-IR (hpIR).

Single knockdowns of all genes tested, excluding *plk2*, *plk3*, and *aurkb*, radiosensitized *p53* mutants with variable efficiency (Figures 1B and 1C). Whereas *atm, atr, smg-1/atx*, and *chk2* deficiencies restored only minor AO reactivity averaging 1%–5% of the $p53^{+/+}$ response, *chk1* knockdown resulted in a staining pattern that closely resembled wild-type (87.7% of the $p53^{+/+}$ response, p < 0.0001; see also Figures 2A and 2B). Enhanced IR-induced cytotoxicity resulted specifically from *chk1* knockdown because (1) injections of a *chk1* mismatch MO failed to radiosensitize *p53* mutants (Figure 2A, bottom panels); (2) the *chk1* MO resulted in a robust reduction of the endogenous Chk1 protein pool, correlating with impaired Chk1 activity (Figure 2C); and (3) a specific inhibitor of human Chk1, but not inhibitors of ATM or Chk2, phenocopied the effects of *chk1* MO (see Figure 7). As would be expected from Chk1 loss, $p53^{e7/e7};chk1^{MO}$ embryos lacked the IR-induced G2/M checkpoint (Figures S1A–S1D). *chk1* MO also fully radiosensitized $p53^{e6}$ ($p53^{N168K}$) homozygotes (Berghmans et al., 2005) and *p53* morphants (Langheinrich et al., 2002) lacking p53 protein (Figure 2E), including in mesodermal derivatives (Figures 2F–2H). Together, these results provide in vivo evidence that Chk1 depletion is sufficient to restore IR sensitivity to *p53* mutant cells.

Transient Chk1 Depletion Is Viable in the Absence of IR

Chk1 is essential for fly and mouse development, with homozygous null mutants succumbing to major cell cycle defects (Fogarty et al., 1997; Liu et al., 2000). We therefore tested whether the cytotoxicity of *chk1* knockdown in zebrafish *p53* mutants was strictly IR dependent. Indeed, *chk1* depletion had no apparent effect on normal zebrafish development and viability, in either the $p53^{+/+}$ or $p53^{e7/e7}$ background (Figures 2A and 2D; compare bars 1 and 2 in Figure 2B). Western blots performed with an anti-zebrafish Chk1 antibody revealed a substantial knockdown of the protein (Figure 2C). Yet *chk1* morphants harbored residual levels of Chk1 activity, as shown by weak but persistent levels of phosphorylated Cdc2 (Figure 2C). These results demonstrate that transient depletion, as opposed to persistent total loss (Liu et al., 2000), of Chk1 function, is tolerable by vertebrate cells in vivo and compatible with long-term organismal viability. Crucially, however (as already shown above), such transient downregulation is sufficient to restore the IR-induced cell-death response in *p53* mutants (Figure 1B, 1C, Figure 2A, and 2B).

Irradiated $p53^{e7/e7};chk1^{MO}$ Embryos Undergo Caspase-3-Independent Cell-Autonomous Apoptosis

Chk1 knockdown might restore a wild-type response to IR (that is, classical intrinsic apoptosis) (Kratz et al., 2006) or trigger a different cell-death program in *p53* mutants. To distinguish between these possibilities, we first analyzed two hallmarks of apoptosis: TUNEL-positive DNA fragmentation and cleaved caspase-3 (as well as electron micrographs) in embryos fixed at 7.5 hpIR. AO labeling of irradiated $p53^{e7/e7};chk1^{MO}$ embryos (Figure 1C and Figure 2A) correlated with high levels of TUNEL labeling throughout the CNS, similar to findings in irradiated $p53^{+/+}$ embryos (Figure 3A). Multiple cells in the irradiated CNS of $p53^{+/+}$ and Chk1-depleted $p53^{e7/e7}$ embryos also showed similar ultrastructural manifestations of apoptosis (e.g., chromatin compaction/segregation and cytoplasmic condensation; Figures 3C and S2). Surprisingly, however, while irradiated $p53^{+/+}$ embryos exhibited strong

immunostaining for active caspase-3, irradiated $p53^{e7/e7};chk1^{MO}$ embryos did not and showed no increase in active caspase-3 levels compared to $p53$ single mutants, which were devoid of both TUNEL and active caspase-3 (Figures 3A and 3B). Thus, the p53-independent cell death-inducing DDR triggered by Chk1 depletion is a caspase-3-independent apoptotic pathway (see also Figure S2F).

To determine the cell autonomy of the Chk1-antagonized pathway, we generated genetic chimeras (Figures 3D and [S3]). While $p53^{e7/e7};chk1^{MO}$ cells grafted into $p53^{e7/e7}$ hosts often stained TUNEL-positive after IR (39%, n = 102), neighboring host cells did not (Figure 3E, upper panels). In the reciprocal experiment, $p53^{e7/e7}$ cells transplanted into $p53^{e7/e7};chk1^{MO}$ hosts remained TUNEL negative within an otherwise TUNEL-positive environment (Figure 3E, lower panels). Therefore, IR-induced TUNEL reactivity of transplanted cells strictly depends on Chk1 dosage, occurs irrespective of the cellular environment, and has very little (if any) influence on neighboring cells. The Chk1-suppressed apoptotic DDR pathway thus functions in a cell-autonomous manner.

Chk1 Blocks a Mitochondria and Death Receptor-Independent Apoptotic Pathway Involving ATM, ATR, and Caspase-2

To molecularly characterize the newly identified apoptotic pathway, we capitalized on the unique advantages of zebrafish embryos for in vivo epistasis analyses. Specifically, we knocked down or forced the expression of candidate pathway contributors in $p53^{e7/e7};chk1^{MO}$ embryos and assessed the effects on IR-induced cell death using the AO assay.

atm and *atr* single knockdowns severely impaired *chk1* knockdown-mediated radiosensitization of zebrafish $p53$ mutants, indicating that ATM and ATR are nonredundantly required to activate the pathway after DNA damage (Figures 4A and 4B; 60% and 90% reductions in cell death levels, respectively). In contrast, single or combined knockdowns of *p63* and/or *p73* led to (at best) a ~30% reduction in AO staining compared to control $p53^{e7/e7};chk1^{MO}$ embryos (Figure 4A). This attenuation was reminiscent of the effects of *chk2* knockdown (Figure S4A, compare bars 3 and 5) and may reflect a role for p53-independent Chk2-p63/p73 apoptotic pathways (Bernassola et al., 2005; Urist et al., 2004) in a subset of cell deaths in irradiated $p53^{e7/e7};chk1^{MO}$ embryos. It is unlikely that these effects result from weaker MO efficiencies, because the *chk2, p63,* and *p73* MOs lead to stronger gene knockdowns than the *atm* and *atr* MOs (Figures 2C and S5A–S5C; also see Rentzsch et al., 2003). The inability of Chk2, p63, and p73 to account for the majority of cell death events in irradiated $p53^{e7/e7};chk1^{MO}$ embryos implies that ATM and ATR operate predominantly within a novel apoptotic pathway, which we have designated "Chk1-suppressed pathway" (CS in Figure 7D).

To test whether the mitochondrial apoptotic axis contributes to the Chk1-suppressed pathway, we first knocked down the proapoptotic BH3-only family member Puma. *puma* depletion did not significantly affect AO labeling of irradiated $p53^{e7/e7};chk1^{MO}$ embryos (Figures 4A and 4B) at a *puma* MO concentration that is otherwise sufficient to completely block IR-induced apoptosis in $p53^{+/+}$ zebrafish embryos (Figure S6) (Kratz et al., 2006). Similarly, a dose of *bcl-xl* mRNA that completely blocked cell death 7.5 hpIR in wild-type embryos failed to affect the AO reactivity of irradiated $p53^{e7/e7};chk1^{MO}$ embryos (Figures 4D and 4E; $p53^{+/+}$ + *bcl-xl*, 0.035% of the mean $p53^{+/+}$ response; $p53^{e7/e7};chk1^{MO}$ + *bcl-xl*, ~95% of the mean $p53^{e7/e7};chk1^{MO}$ response). *casp9* knockdown also lacked an effect (Figures 4A, 4B, and S5E). Thus, two major regulators of mitochondrial membrane permeabilization (Puma and Bcl-x_L), as well as the main initiator and executioner caspases acting downstream of mitochondria (caspase-9 and caspase-3, see Figure 3), are dispensable for the Chk1-suppressed apoptotic pathway.

The death-receptor axis bypasses the requirement for mitochondria and caspase-9, suggesting that it could contribute to the Chk1-suppressed pathway. In addition, a link between Chk1 loss and caspase-8 activation has recently been observed (Xiao et al., 2005). Even so, the death-receptor pathway converges on caspase-3 activation via caspase-8 (Hengartner, 2000). This caspase-3 recruitment contrasts with the caspase-3 independence of the pathway we identified, which, together with the established cell autonomy of the new pathway (Figure 3E), argues against a role for DNA damage-induced extrinsic signaling downstream of *chk1* depletion. Indeed, the AO reactivity of $p53^{e7/e7};chk1^{MO};casp8^{MO}$ zebrafish embryos did not differ from that of $p53^{e7/e7};chk1^{MO}$ specimens (Figures 4A and ^{S5D}). Blocking death-receptor signaling with a *fadd* (Fas Associated protein with Death Domain) MO (Eimon et al., 2006) also failed to affect AO staining (Figure 4A). Thus, extrinsic signaling—like mitochondrial signaling— does not appear to play an important role downstream of *chk1* loss.

The sole caspase whose depletion blocked the Chk1-suppressed pathway was caspase-2, a poorly characterized yet highly conserved caspase with features of both initiator and executioner caspases (Zhivotovsky and Orrenius, 2005). In three separate experiments, $p53^{e7/e7};chk1^{MO};casp2^{MO1}$ embryos consistently showed a mean 6-fold decrease in AO labeling compared with $p53^{e7/e7};chk1^{MO}$ embryos (~16% of the mean $p53^{e7/e7};chk1^{MO}$ response, $p < 0.0001$; Figures 4A and 4B). *casp2* MO1, which targets the splice donor site of intron 4, led to marked reductions in *casp2* mRNA levels and to aberrant residual transcripts lacking exon 4 (Figure 4C). A second *casp2* MO reduced IR-induced death in $p53^{e7/e7};chk1^{MO}$ embryos (Figure S5F and S5G), and a mismatch version of *casp2* MO1 had no effect (data not shown). Altogether, these epistasis analyses identify a novel *atm/atr-casp2* apoptotic program as a key mechanism through which Chk1 depletion radiosensitizes *p53* mutant zebrafish embryos without recruiting the classical mitochondrial and death-receptor pathways (Figure 7D).

The Chk1-Suppressed Apoptotic Pathway Is Conserved In Human Cancer Cells

We next investigated whether the DNA damage-induced apoptotic pathway suppressed by Chk1 in zebrafish is conserved in human cancer cells defective in p53 signaling. To inhibit Chk1 in these cells, we used the indolocarbazole small molecule Gö6976 (Kohn et al., 2003), which has greater specificity than the commonly used Chk1 inhibitor UCN-01 (reviewed in Kawabe, 2004 and see below). In HeLa cells (in which the p53 protein pool is depleted by HPV-18 E6), caspase-2 cleavage was readily apparent at 24 hpIR in the presence of Gö6976 (Figure 5A). This effect was synergistic because neither IR nor Gö6976 alone caused substantial increases in cleaved caspase-2 levels compared to basal levels observed in control cells. In addition, caspase-2 cleavage tightly correlated with a strong radiosensitizing effect (~50% increase in cell death; Figure 5B, compare bars 5 and 6; see also Figure 5J, 5K, and Figure 6C). By contrast, the levels of cleaved caspase-3 in Gö6976-treated cells at 24 hpIR were negligible and did not differ from those observed in irradiated cells not exposed to the inhibitor (Figure 5A). Furthermore, both caspase-2 cleavage and concomitant cellular radiosensitization were insensitive to overexpression of human *BCL2*, whereas caspase-3 cleavage was completely removed in this context (Figures 5A and 5B, compare bars 7 and 8). Synergistic activation of caspase-2 by Gö6976 and IR did not elicit or involve cytochrome *c* release from the mitochondria at 24 hpIR (Figure 5C). Together, these findings demonstrate that Chk1 inhibition and IR synergize to activate caspase-2 and trigger *BCL2*- and mitochondria-independent cell death in p53-defective human cells, consistent with our zebrafish data.

Before testing whether caspase-2 is required for cell-death induction, we verified the specificity of Gö6976 as an inhibitor of Chk1. *CHK1* siRNA, but not a *LACZ* control siRNA, induced caspase-2 cleavage in concert with IR at 24 hr posttreatment but did not stimulate caspase-3

processing at this stage, in accord with the effects of Gö6976 (Figure 5D). Furthermore, while Gö6976 inhibited Chk1 in a dose-dependent manner, it did not impair MK-2 activity (Figure 5E), in contrast with UCN-01 (Reinhardt et al., 2007).

To test whether caspase-2 is required for Gö6976-mediated HeLa cell killing after IR, we used three independent *CASP2* shRNAs that produced strong and specific knockdowns (Figure 5G). Each shRNA significantly reduced apoptosis induction at 48 hr after IR + Gö6976 treatment, but not after IR treatment alone (Figure 5H; see also Figures 5J and 5K). In contrast, the reduction in apoptosis observed upon *CASP3* knockdown at 48 hr (stage at which caspase-3 is eventually cleaved) was independent of Gö6976, as *CASP3* shRNA led to a similar attenuation after IR treatment alone (Figure 5H). The severity of the apoptotic blockades caused by the *CASP2* shRNAs (20%–45% reductions, p < 0.01 for each) correlated with their respective knockdown efficiencies (Figures 5G and 5H). Altogether, these results demonstrate that caspase-2—but not caspase-3—is specifically required for the increase in IR-induced apoptosis observed in Chk1-inhibited human cancer cells, similar to its requirement in irradiated $p53^{e7/e7};chk1^{MO}$ zebrafish embryos.

If the ATM/ATR-caspase-2 apoptotic axis in zebrafish is well conserved in human cells, ATM and ATR should be activated after Chk1 inhibition in irradiated HeLa cells, similar to caspase-2. Indeed, IR + Gö6976 treatment led to synergistic increases in phosphorylated Chk2 at Thr68 (readout for ATM activity) and phosphorylated Chk1 at Ser317 (readout for ATR activity) (Figure 5I). Elevated ATM and ATR activities correlated with increased levels of DNA damage in the IR + Gö6976-treated cells, as indicated by an increased abundance of phosphorylated H2A.X (Figure 5I). Even though Chk2 was strongly activated in this context (Figure 5I), a specific *CHK2* siRNA failed to block caspase-2 activation (Figures S4B and S4C). This result substantiates our prediction (based on epistasis analyses in zebrafish) that the Chk1-suppressed pathway is Chk2 independent. Taken together, our experiments in HeLa cells show that apoptosis after IR + Gö6976 treatment of human cells involves ATM and ATR activation, is independent of Chk2, Bcl-2, mitochondria, and caspase-3, but requires caspase-2 activation and function (Figure 7D). Thus, the zebrafish Chk1-suppressed pathway is evolutionarily conserved in human cancer cells.

Chk1 Inhibition Induces a Sustained Increase in S Phase Apoptosis after IR

MK-2 depleted $Tp53^{-/-}$ MEFs (mouse embryonic fibroblasts) undergo DNA damage-induced apoptosis exclusively during mitosis (Reinhardt et al., 2007). In contrast, pH3/TUNEL double-labeling of irradiated $p53^{e7/e7};chk1^{MO}$ zebrafish embryos indicates that Chk1-suppressed apoptosis operates predominantly during the cell-cycle interphase (Figure S7). To further address this question in HeLa cells, we used TUNEL/PI double labeling, such that PI fluorescence intensity indicated the cell-cycle status of TUNEL-positive cells. The Chk1-suppressed pathway was readily detected in this assay as a dramatic, entirely caspase-2-dependent increase in TUNEL-positive cells after IR + Gö6976 treatment (Figures 5J and 5K). Moreover, the cell-cycle distribution of TUNEL-positive cells was significantly different upon IR + Gö6976 treatment compared to IR alone. Whereas only a minority of TUNEL-positive cells were in G1 or S phase in the presence of normal Chk1 activity (~15% each), these fractions increased 2.5-fold upon Chk1 inhibition (~35% and ~40% of TUNEL-positive cells, respectively; p < 0.002 for each) (Figure 5L). Thus, in human cells, the Chk1-suppressed pathway operates predominantly during the S and G1 phases of the cell cycle. Importantly, Gö6976-induced S phase apoptosis increased with time and the effect was sustained for at least 72 hpIR (Figure S8), indicating an important role for Chk1 in preventing DNA damage-induced apoptosis during DNA replication (see Discussion).

Chk1 Inhibition Sensitizes Multiple Cancer Cell Lines to IR-Induced Apoptosis

We next asked whether the Chk1-suppressed pathway could be triggered in human cancer cell lines other than HeLa, including $TP53^{+/+}$ and $TP53^{-/-}$ HCT116 colon carcinoma cells (Bunz et al., 1998), the SAOS2 osteosarcoma line (p53 null), the MDA-MB-435 breast cancer line (heterozygous for the G266E mutation), and the V173M/R282W, transheterozygous LN-428 glioblastoma line (Ishii et al., 1999). All $TP53$ null or mutant lines tested displayed increases in caspase-2 cleavage and apoptosis after IR + Gö6976 treatment (Figures 6A–6C). While these observations substantiate the results in HeLa cells, we noted several differences. First, $TP53^{+/+}$ HCT116 cells failed to engage the Chk1-suppressed pathway, as evidenced by their inability to cleave caspase-2 after IR + Gö6976 treatment (see also Discussion). Instead, caspase-3 was activated in a p53-dependent manner (likely via classical mitochondrial signaling), followed by a modest increase in apoptosis. Intriguingly, $TP53$ mutant MDA-MB-435 and LN-428 cells also engaged caspase-3 cleavage after IR + Gö6976 treatment (Figure 6B). This caspase-3 cleavage could result from either p53-independent apoptotic processes operating in parallel with the newly identified pathway (such as the Chk2-p63/73 axis), or from caspase-2 itself triggering the classical intrinsic or extrinsic apoptotic pathways (dashed arrows in Figure 7D) (Castedo et al., 2004b; Nutt et al., 2005; Shin et al., 2005; Tu et al., 2006; Zhivotovsky and Orrenius, 2005). However, it is unlikely that any of these alternative pathways substitute for the Chk1-suppressed pathway in HeLa, SAOS2, or $TP53^{-/-}$ HCT116 lines, in which caspase-3 cleavage is undetectable or minimal after IR + Gö6976 treatment (Figure 5A, Figure 6A, and 6B).

Gö6976 Selectively Radiosensitizes Zebrafish In Vivo Models of *p53* Loss and *bcl-2* Gain

To investigate the effects of Gö6976 in vivo, we evaluated it—together with specific Chk2 and ATM inhibitors—in the zebrafish system. Drug toxicity was monitored by scoring the AO reactivity of inhibitor-treated, but nonirradiated, $p53^{+/+}$ embryos (left column in Figure 7A). Unless otherwise indicated, the inhibitors were applied at 17 hpf (1 hr before IR) for a total of 6 hr.

Whereas relatively toxic doses of KU55933 (an ATM inhibitor) (Hickson et al., 2004) and Chk2 Inhibitor II (Arienti et al., 2005) only modestly radiosensitized *p53* mutants, a nontoxic dose of Gö6976 (1 µM) restored a complete apoptotic response to IR (Figure 7A). The effects of Gö6976 were almost fully penetrant, with 95% of Gö6976-treated *p53* mutants (n = 210) showing a marked IR-induced apoptotic response. In fact, as short as a 1.5 hr exposure to Gö6976 immediately after IR was sufficient to phenocopy the 0–24 hpf *chk1* depletion obtained via *chk1* MO (Figure 7B). Similar to *chk1* morphants, nonirradiated $p53^{+/+}$ embryos treated with Gö6976 developed into normal adults without overt signs of spontaneous tumorigenesis or other pathologies.

The *BCL2/XL* independence of the Chk1-suppressed pathway (Figure 4D and Figure 5B) suggests that Chk1 inhibitors could prove valuable in radio/chemosensitizing malignancies that overexpress *BCL2* family members, including follicular lymphoma. *Tg(rag2: EGFP-bcl-2)* larvae are characterized by highly radioresistant T and B cells at 9 dpf (Langenau et al., 2005). Systemic treatment with Gö6976 suppressed T cell radioresistance in a mean 58% of these larvae (n = 26) compared to none of the DMSO-treated larvae (n = 28), without any apparent adverse effects (Figure 7C). Together with our human cell culture studies, the in vivo analysis of Gö6976 in zebrafish supports the concept that human tumors with mutational alteration of p53 or its attendant downstream pathway—in other words, most human cancers—would be selectively sensitized by Chk1 inhibitors to DNA damage-induced apoptosis.

DISCUSSION

We have identified an evolutionarily conserved apoptotic process distinct from the mitochondrial and death-receptor axes. This ATM/ATR-caspase-2 pathway is triggered by DNA damage in cells in which Chk1 activity is simultaneously compromised. The pathway is insensitive to p53 loss and *BCL2/XL* gain—two of the most common genetic abnormalities in human cancers—can be targeted with Chk1 inhibitors and assessed on the basis of caspase-2 cleavage.

The ATM/ATR-caspase-2 pathway is triggered by the combined effects of IR and Chk1 inhibition, but not by either stimulus alone. Our data show increased levels of γH2A.X and synergistic activation of ATM and ATR in irradiated cells lacking Chk1, indicating that Chk1 acts upstream of ATM and ATR to moderate the accumulation of DNA damage. This might suggest that increasing IR doses would eventually substitute for Chk1 inhibitor treatment by matching a DNA-damage threshold necessary for caspase-2 activation. However, even very high levels of DNA damage induced by IR doses of up to 150 Gy (Gray) did not robustly induce apoptosis in zebrafish *p53* mutants with functional Chk1 (Figure S10). Thus, the ATM/ATR-caspase-2 pathway cannot mount a nonspecific response to excess damage, but rather is obligatorily tied to Chk1 activity. An involvement of Chk1's essential or damage-dependent checkpoint functions during DNA replication (Bartek et al., 2004; Lam et al., 2004; Sorensen et al., 2003; Syljuasen et al., 2005) seems likely given the sustained rise in S phase apoptosis observed in IR + Chk1 inhibitor-treated HeLa cells. A role for replication stress in triggering the ATM/ATR-caspase-2 pathway gains support from observations that Chk1-depleted cells exposed to replication inhibitors undergo p53- and Chk2-independent apoptosis during S phase (Rodríguez and Meuth, 2006). Also, caspase-2 is the sole caspase whose proform resides in the nucleus (Zhivotovsky et al., 1999), where it is stabilized by cyclin D3, a positive regulator of the G1/S transition (Mendelsohn et al., 2002). We propose that tight control of the ATM/ATR-caspase-2 pathway by Chk1 contributes to the decision to live (arrest and repair) or die in replicating cells suffering DNA damage.

ATM and ATR, while both necessary for activation of the Chk1-suppressed pathway, are individually insufficient for this function (Figure 4A). ATM and ATR might phosphorylate different substrates, each being essential for caspase-2 activation and susceptible to Chk1 regulation. However, neither caspase-2 nor its proposed activators, including PIDDosome components PIDD (p53-induced protein with death domain) and RAIDD (RIP-associated ICH-1/CED-3 homologous protein with a death domain) (Tinel and Tschopp, 2004), belong to the list of 700 potential ATM/ATR substrates (Matsuoka et al., 2007). A more likely interpretation is that ATM and ATR serve different sensory functions, with ATM responding primarily to IR-induced double-strand breaks while ATR predominantly senses signals resulting from reduced Chk1 activity, such as replication stress (Cuadrado et al., 2006; Syljuasen et al., 2005).

The ATM/ATR-caspase-2 pathway may serve as a mechanism that ensures the demise of cells carrying potentially harmful DNA lesions in the absence of proper genome-surveillance activity (as provided by Chk1) (Lam et al., 2004). Such a function might help explain why *CHK1* mutations, despite fueling genomic instability (Lam et al., 2004), are paradoxically rare in human cancers (Bartek and Lukas, 2003). Our demonstration that the Chk1-suppressed pathway can operate in both the absence and presence of p53, as revealed in irradiated *p53*^{+/+}*;chk1*[MO]*;bcl-xl* embryos and in irradiated *p53*^{+/+}*;Tg(rag2:EGFP-bcl-2)* larvae treated with Gö6976, disqualifies it as a "backup" program (Roos and Kaina, 2006) operating only in cells that lack p53. Rather, we propose that it constitutes an alternative, perhaps primitive, response to DNA injury that evolved independently of the p53 network. Intriguingly, however, *TP53*^{+/+} and *TP53*^{−/−} HCT116 cells differed in their response to IR + Gö6976 treatment, in

that caspase-2 but not caspase-3 cleavage was actively inhibited in the $TP53^{+/+}$ cells, via an apparent downregulation of procaspase-2 levels (Figure 6A; see also Baptiste-Okoh et al., 2008). Thus, a form of crosstalk might have evolved to link these p53-dependent and -independent apoptotic pathways, similar to that described for caspase-dependent and -independent pathways (Colell et al., 2007).

Chk1 inhibitors can radio/chemosensitize *p53*-deficient human tumor cells in vitro, leading to clinical trials of their activity in cancer patients (Kawabe, 2004; Tse et al., 2007; Zhou and Bartek, 2004). Because of the embryonic lethality of $Chk1^{-/-}$ mice, however, it has remained unclear whether the potency and selectivity of radio/chemosensitization observed in vitro will apply in vivo. Our findings in zebrafish using the Chk1 inhibitor Gö6976 and *chk1* morphants, which retain residual levels of Chk1 activity, indicate that levels of Chk1 inhibition not toxic to normal cells are sufficient to sensitize *p53* mutant cells to IR-induced apoptosis within a living vertebrate. Our results also identify cleavage of caspase-2 as a candidate biomarker for Chk1-targeting treatments. The isolation of such specific biomarkers remains a pressing challenge in the development and optimal use of targeted cancer therapeutics (Cully et al., 2006; Tse et al., 2007). Finally, our results unexpectedly predict that in addition to tumors with altered p53 activity, those with other types of prosurvival alterations that block mitochondrial signaling downstream of p53, such as *BCL2*-expressing follicular lymphomas, would respond favorably to combination therapy with Chk1 inhibitors.

EXPERIMENTAL PROCEDURES

Zebrafish Stocks

The homozygous viable $p53^{M214K}$ and $p53^{N168K}$ mutant lines ($p53^{e7}$ and $p53^{e6}$, respectively, in this article) (Berghmans et al., 2005), and the *Tg(rag2:GFP)* (Langenau et al., 2003), *Tg (rag2:EGFP-bcl-2)* (Langenau et al., 2005), *Tg(pu. 1:GFP)* (Hsu et al., 2004), and *Tg (myoD:EGFP)* (Yang et al., 2004) transgenic lines were used and maintained at 28.5°C by standard methods. For experimental purposes, irradiated $p53^{e6/e6}$ embryos were incubated for 6 hr at 37°C (restrictive temperature for *N168K*).

Morpholino Screen and Epistasis Analyses Using the Live AO Assay

MOs were obtained from Gene Tools, LLC. MO sequences, target sites, working concentrations, knockdown efficiencies, selected references, and injection procedures, as well as detailed protocols for AO staining of live embryos and the ImageJ-based quantification method, are listed in Table S1, Figure S5, and the Supplemental Experimental Procedures.

Human Cancer Cell Lines, siRNAs, and shRNAs

The HeLa, SAOS2, MDA-MB-435, and LN-428 cell lines, the $TP53^{+/+}$ and $TP53^{-/-}$ HCT116 isogenic pair (Bunz et al., 1998), and the *Cyt-c-GFP* transgenic, 2H18 HeLa-derived lines (Goldstein et al., 2000), carrying or not carrying a *BCL2* transgene, were cultured in DMEM medium (GIBCO) supplemented with 15% fetal bovine serum (FBS). siRNAs were transfected in HeLa cells using Hiperfect (QIAGEN) according to the manufacturer's instructions. Cells were exposed to IR +/− Gö6976 at 48 or 72 hr posttransfection. shRNA knockdown analyses were performed as previously described (Moffat et al., 2006). See Supplemental Data for more details, siRNA and shRNA sequences, and all other experimental procedures.

ACKNOWLEDGMENTS

REFERENCES

Afshar G, Jelluma N, Yang X, Basila D, Arvold ND, Karlsson A, Yount GL, Dansen TB, Koller E, Haas-Kogan DA. Radiation-induced caspase-8 mediates p53-independent apoptosis in glioma cells. Cancer Res 2006;66:4223–1232. [PubMed: 16618745]

Arienti KL, Brunmark A, Axe FU, McClure K, Lee A, Blevitt J, Neff DK, Huang L, Crawford S, Pandit CR, et al. Checkpoint kinase inhibitors: SAR and radioprotective properties of a series of 2-arylbenzimidazoles. J. Med. Chem 2005;48:1873–1885. [PubMed: 15771432]

Baptiste-Okoh N, Barsotti AM, Prives C. Caspase 2 is both required for p53-mediated apoptosis and downregulated by p53 in a p21-dependent manner. Cell Cycle 2008;7Published online February 19, 2008.

Bartek J, Lukas J. Chk1 and Chk2 kinases in checkpoint control and cancer. Cancer Cell 2003;3:421–429. [PubMed: 12781359]

Bartek J, Lukas C, Lukas J. Checking on DNA damage in S phase. Nat. Rev. Mol. Cell Biol 2004;5:792–804. [PubMed: 15459660]

Berghmans S, Murphey RD, Wienholds E, Neuberg D, Kutok JL, Fletcher CD, Morris JP, Liu TX, Schulte-Merker S, Kanki JP, et al. tp53 mutant zebrafish develop malignant peripheral nerve sheath tumors. Proc. Natl. Acad. Sci. USA 2005;102:407–412. [PubMed: 15630097]

Bernassola F, Oberst A, Melino G, Pandolfi PP. The promyelocytic leukaemia protein tumour suppressor functions as a transcriptional regulator of p63. Oncogene 2005;24:6982–6986. [PubMed: 16007146]

Bunz F, Dutriaux A, Lengauer C, Waldman T, Zhou S, Brown JP, Sedivy JM, Kinzler KW, Vogelstein B. Requirement for p53 and p21 to sustain G2 arrest after DNA damage. Science 1998;282:1497–1501. [PubMed: 9822382]

Castedo M, Perfettini JL, Roumier T, Andreau K, Medema R, Kroemer G. Cell death by mitotic catastrophe: a molecular definition. Oncogene 2004a;23:2825–2837. [PubMed: 15077146]

Castedo M, Perfettini JL, Roumier T, Yakushijin K, Horne D, Medema R, Kroemer G. The cell cycle checkpoint kinase Chk2 is a negative regulator of mitotic catastrophe. Oncogene 2004b;23:4353–4361. [PubMed: 15048074]

Colell A, Ricci JE, Tait S, Milasta S, Maurer U, Bouchier-Hayes L, Fitzgerald P, Guio-Carrion A, Waterhouse NJ, Li CW, et al. GAPDH and autophagy preserve survival after apoptotic cytochrome c release in the absence of caspase activation. Cell 2007;129:983–997. [PubMed: 17540177]

Cuadrado M, Martinez-Pastor B, Fernandez-Capetillo O. "ATR activation in response to ionizing radiation: still ATM territory.". Cell Div 2006;1:7. [PubMed: 16759429]

Cully M, You H, Levine AJ, Mak TW. Beyond PTEN mutations: the PI3K pathway as an integrator of multiple inputs during tumorigenesis. Nat. Rev. Cancer 2006;6:184–192. [PubMed: 16453012]

Eimon PM, Kratz E, Varfolomeev E, Hymowitz SG, Stern H, Zha J, Ashkenazi A. Delineation of the cell-extrinsic apoptosis pathway in the zebrafish. Cell Death Differ 2006;13:1619–1630. [PubMed: 16888647]

Fogarty P, Campbell SD, Abu-Shumays R, Phalle BS, Yu KR, Uy GL, Goldberg ML, Sullivan W. The Drosophila grapes gene is related to checkpoint gene chk1/rad27 and is required for late syncytial division fidelity. Curr. Biol 1997;7:418–426. [PubMed: 9197245]

Frenkel J, Sherman D, Fein A, Schwartz D, Almog N, Kapon A, Goldfinger N, Rotter V. Accentuated apoptosis in normally developing p53 knockout mouse embryos following genotoxic stress. Oncogene 1999;18:2901–2907. [PubMed: 10362261]

Goldstein JC, Waterhouse NJ, Juin P, Evan GI, Green DR. The coordinate release of cytochrome c during apoptosis is rapid, complete and kinetically invariant. Nat. Cell Biol 2000;2:156–162. [PubMed: 10707086]

Gong JG, Costanzo A, Yang HQ, Melino G, Kaelin WG Jr, Levrero M, Wang JY. The tyrosine kinase c-Abl regulates p73 in apoptotic response to cisplatin-induced DNA damage. Nature 1999;399:806–809. [PubMed: 10391249]

Hengartner MO. The biochemistry of apoptosis. Nature 2000;407:770–776. [PubMed: 11048727]

Hickson I, Zhao Y, Richardson CJ, Green SJ, Martin NM, Orr AI, Reaper PM, Jackson SP, Curtin NJ, Smith GC. Identification and characterization of a novel and specific inhibitor of the ataxia-telangiectasia mutated kinase ATM. Cancer Res 2004;64:9152–9159. [PubMed: 15604286]

Hsu K, Traver D, Kutok JL, Hagen A, Liu TX, Paw BH, Rhodes J, Berman JN, Zon LI, Kanki JP, et al. The pu.1 promoter drives myeloid gene expression in zebrafish. Blood 2004;104:1291–1297. [PubMed: 14996705]

Huang H, Regan KM, Lou Z, Chen J, Tindall DJ. CDK2-dependent phosphorylation of FOXO1 as an apoptotic response to DNA damage. Science 2006;314:294–297. [PubMed: 17038621]

Ishii N, Maier D, Merlo A, Tada M, Sawamura Y, Diserens AC, Van Meir EG. Frequent co-alterations of TP53, p16/CDKN2A, p14ARF, PTEN tumor suppressor genes in human glioma cell lines. Brain Pathol 1999;9:469–479. [PubMed: 10416987]

Kasibhatla S, Brunner T, Genestier L, Echeverri F, Mahboubi A, Green DR. DNA damaging agents induce expression of Fas ligand and subsequent apoptosis in T lymphocytes via the activation of NF-kappa B and AP-1. Mol. Cell 1998;1:543–551. [PubMed: 9660938]

Kawabe T. G2 checkpoint abrogators as anticancer drugs. Mol. Cancer Ther 2004;3:513–519. [PubMed: 15078995]

Kohn EA, Yoo CJ, Eastman A. The protein kinase C inhibitor Gö6976 is a potent inhibitor of DNA damage-induced S and G2 cell cycle checkpoints. Cancer Res 2003;63:31–35. [PubMed: 12517773]

Kolesnick R, Fuks Z. Radiation and ceramide-induced apoptosis. Oncogene 2003;22:5897–5906. [PubMed: 12947396]

Kratz E, Eimon PM, Mukhyala K, Stern H, Zha J, Strasser A, Hart R, Ashkenazi A. Functional characterization of the Bcl-2 gene family in the zebrafish. Cell Death Differ 2006;13:1631–1640. [PubMed: 16888646]

Lam MH, Liu Q, Elledge SJ, Rosen JM. Chk1 is haploinsufficient for multiple functions critical to tumor suppression. Cancer Cell 2004;6:45–59. [PubMed: 15261141]

Langenau DM, Traver D, Ferrando AA, Kutok JL, Aster JC, Kanki JP, Lin S, Prochownik E, Trede NS, Zon LI, et al. Myc-induced T cell leukemia in transgenic zebrafish. Science 2003;299:887–890. [PubMed: 12574629]

Langenau DM, Jette C, Berghmans S, Palomero T, Kanki JP, Kutok JL, Look AT. Suppression of apoptosis by bcl-2 overexpression in lymphoid cells of transgenic zebrafish. Blood 2005;105:3278–3285. [PubMed: 15618471]

Langheinrich U, Hennen E, Stott G, Vacun G. Zebrafish as a model organism for the identification and characterization of drugs and genes affecting p53 signaling. Curr. Biol 2002;12:2023–2028. [PubMed: 12477391]

Li H, Kolluri SK, Gu J, Dawson MI, Cao X, Hobbs PD, Lin B, Chen G, Lu J, Lin F, et al. Cytochrome c release and apoptosis induced by mitochondrial targeting of nuclear orphan receptor TR3. Science 2000;289:1159–1164. [PubMed: 10947977]

Lin B, Kolluri SK, Lin F, Liu W, Han YH, Cao X, Dawson MI, Reed JC, Zhang XK. Conversion of Bcl-2 from protector to killer by interaction with nuclear orphan receptor Nur77/TR3. Cell 2004;116:527–540. [PubMed: 14980220]

Liu Q, Guntuku S, Cul XS, Matsuoka S, Cortez D, Tamai K, Luo G, Carattini-Rivera S, DeMayo F, Bradley A, et al. Chk1 is an essential kinase that is regulated by Atr and required for the G(2)/M DNA damage checkpoint. Genes Dev 2000;14:1448–1459. [PubMed: 10859164]

Matsuoka S, Ballif BA, Smogorzewska A, McDonald ER 3rd, Hurov KE, Luo J, Bakalarski CE, Zhao Z, Solimini N, Lerenthal Y, et al. ATM and ATR substrate analysis reveals extensive protein networks responsive to DNA damage. Science 2007;316:1160–1166. [PubMed: 17525332]

Mendelsohn AR, Hamer JD, Wang ZB, Brent R. Cyclin D3 activates Caspase 2, connecting cell proliferation with cell death. Proc. Natl. Acad. Sci. USA 2002;99:6871–6876. [PubMed: 12011445]

Moffat J, Grueneberg DA, Yang X, Kim SY, Kloepfer AM, Hinkle G, Piqani B, Eisenhaure TM, Luo B, Grenier JK, et al. A lentiviral RNAi library for human and mouse genes applied to an arrayed viral high-content screen. Cell 2006;124:1283–1298. [PubMed: 16564017]

Nutt LK, Margolis SS, Jensen M, Herman CE, Dunphy WG, Rathmell JC, Kornbluth S. Metabolic regulation of oocyte cell death through the CaMKII-mediated phosphorylation of caspase-2. Cell 2005;123:89–103. [PubMed: 16213215]

Pyati UJ, Look AT, Hammerschmidt M. Zebrafish as a powerful vertebrate model system for in vivo studies of cell death. Semin. Cancer Biol 2007;17:154–165. [PubMed: 17210257]

Reinhardt HC, Aslanian AS, Lees JA, Yaffe MB. p53-deficient cells rely on ATM- and ATR-mediated checkpoint signaling through the p38MAPK/MK2 pathway for survival after DNA damage. Cancer Cell 2007;11:175–189. [PubMed: 17292828]

Rentzsch F, Kramer C, Hammerschmidt M. Specific and conserved roles of TAp73 during zebrafish development. Gene 2003;323:19–30. [PubMed: 14659876]

Rodríguez R, Meuth M. Chk1 and p21 cooperate to prevent apoptosis during DNA replication fork stress. Mol. Biol. Cell 2006;17:402–412. [PubMed: 16280359]

Roos WP, Kaina B. DNA damage-induced cell death by apoptosis. Trends Mol. Med 2006;12:440–450. [PubMed: 16899408]

Shin S, Lee Y, Kim W, Ko H, Chol H, Kim K. Caspase-2 primes cancer cells for TRAIL-mediated apoptosis by processing procaspase-8. EMBO J 2005;24:3532–3542. [PubMed: 16193064]

Sorensen CS, Syljuasen RG, Falck J, Schroeder T, Ronnstrand L, Khanna KK, Zhou BB, Bartek J, Lukas J. Chk1 regulates the S phase checkpoint by coupling the physiological turnover and ionizing radiation-induced accelerated proteolysis of Cdc25A. Cancer Cell 2003;3:247–258. [PubMed: 12676583]

Syljuasen RG, Sorensen CS, Hansen LT, Fugger K, Lundin C, Johansson F, Helleday T, Sehested M, Lukas J, Bartek J. Inhibition of human Chk1 causes increased initiation of DNA replication, phosphorylation of ATR targets, and DNA breakage. Mol. Cell. Biol 2005;25:3553–3562. [PubMed: 15831461]

Tinel A, Tschopp J. The PIDDosome, a protein complex implicated in activation of caspase-2 in response to genotoxic stress. Science 2004;304:843–846. [PubMed: 15073321]

Tse AN, Carvajal R, Schwartz GK. Targeting checkpoint kinase 1 in cancer therapeutics. Clin. Cancer Res 2007;13:1955–1960. [PubMed: 17404075]

Tu S, McStay GP, Boucher LM, Mak T, Beere HM, Green DR. In situ trapping of activated initiator caspases reveals a role for caspase-2 in heat shock-induced apoptosis. Nat. Cell Biol 2006;8:72–77. [PubMed: 16362053]

Urist M, Tanaka T, Poyurovsky MV, Prives C. p73 induction after DNA damage is regulated by checkpoint kinases Chk1 and Chk2. Genes Dev 2004;18:3041–3054. [PubMed: 15601819]

Vousden KH, Lu X. Live or let die: the cell's response to p53. Nat. Rev. Cancer 2002;2:594–604. [PubMed: 12154352]

Wichmann A, Jaklevic B, Su TT. Ionizing radiation induces caspase-dependent but Chk2- and p53-independent cell death in Drosophila melanogaster. Proc. Natl. Acad. Sci. USA 2006;103:9952–9957. [PubMed: 16785441]

Xiao Z, Xue J, Sowln TJ, Rosenberg SH, Zhang H. A novel mechanism of checkpoint abrogation conferred by Chk1 downregulation. Oncogene 2005;24:1403–1411. [PubMed: 15608676]

Yang HW, Kutok JL, Lee NH, Piao HY, Fletcher CD, Kanki JP, Look AT. Targeted expression of human MYCN selectively causes pancreatic neuroendocrine tumors in transgenic zebrafish. Cancer Res 2004;64:7256–7262. [PubMed: 15492244]

Yount GL, Afshar G, Ries S, Korn M, Shalev N, Basila D, McCormick F, Haas-Kogan DA. Transcriptional activation of TRADD mediates p53-independent radiation-induced apoptosis of glioma cells. Oncogene 2001;20:2826–2835. [PubMed: 11420694]

Yuan ZM, Shioya H, Ishiko T, Sun X, Gu J, Huang YY, Lu H, Kharbanda S, Weikchselbaum R, Kufe D. p73 is regulated by tyrosine kinase c-Abl in the apoptotic response to DNA damage. Nature 1999;399:814–817. [PubMed: 10391251]

Zhivotovsky B, Orrenius S. Caspase-2 function in response to DNA damage. Biochem. Biophys. Res. Commun 2005;331:859–867. [PubMed: 15865942]

Zhivotovsky B, Samali A, Gahm A, Orrenius S. Caspases: their intracellular localization and translocation during apoptosis. Cell Death Differ 1999;6:644–651. [PubMed: 10453075]

Zhou BB, Bartek J. Targeting the checkpoint kinases: chemosensitization versus chemoprotection. Nat. Rev. Cancer 2004;4:216–225. [PubMed: 14993903]
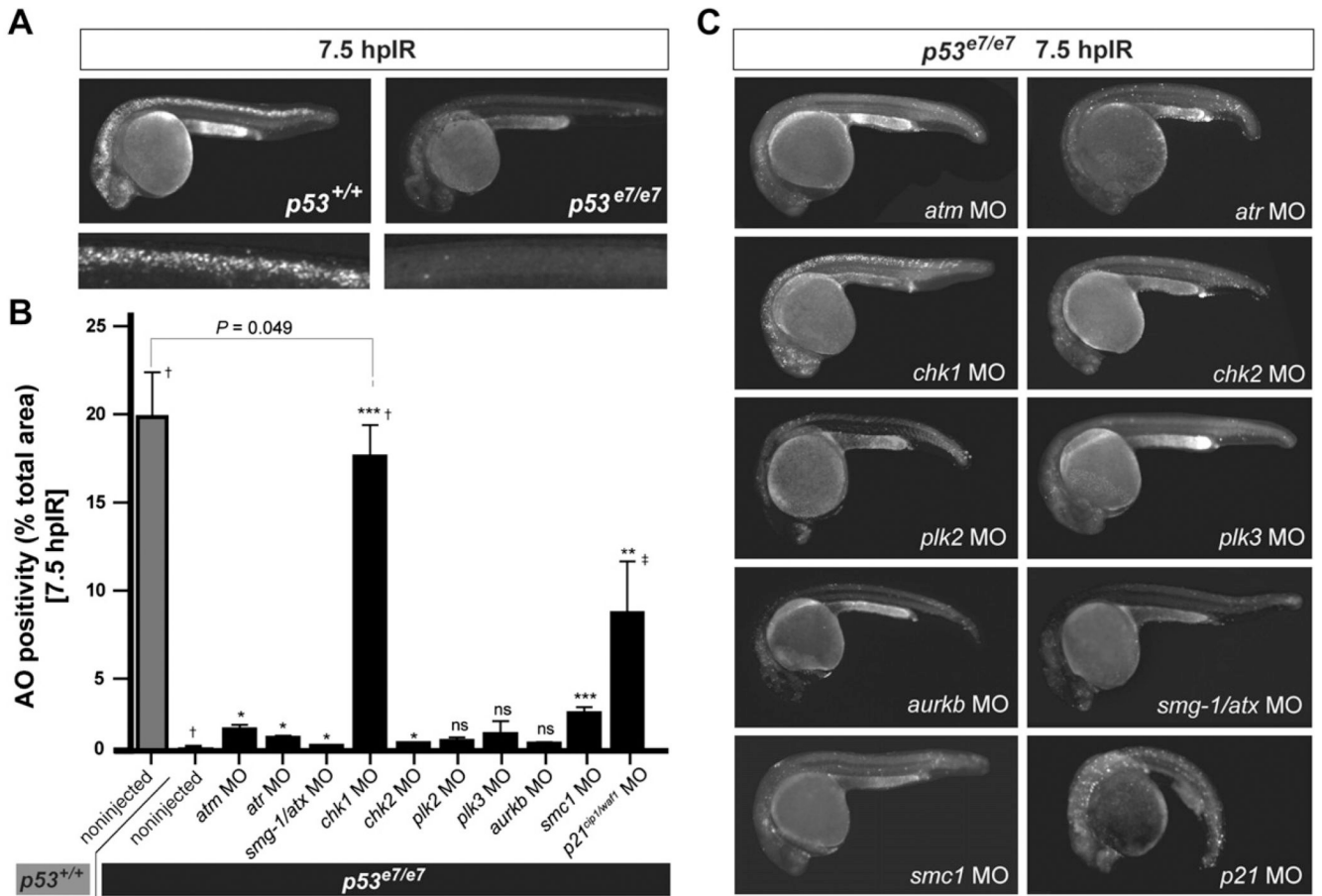
Figure 1. A Morpholino Screen Identifies *chk1* as a Loss-of-Function Suppressor of *p53^{e7/e7}*-Associated Radioresistance

(A) Live 25 hpf embryos of the indicated genotypes stained with AO at 7.5 hpIR (12.5 Gy). Anterior, left. Note the complete absence of AO labeling in the brain and spinal cord of the irradiated *p53* mutant.

(B) MO screen for loss-of-function suppressors of *p53^{e7/e7}*-associated radioresistance. Noninjected and 1 cell-stage MO-injected embryos were irradiated at 18 hpf (12.5 Gy). AO uptake by cells was quantified by analyzing images of whole embryos photographed live at 7.5 hpIR (y axis) (images as in C). Injected MOs are indicated along the x axis. Bars are color coded and refer to the genetic background used for injections (gray, *p53^{+/+}*; black, *p53^{e7/e7}*). AO staining was quantified in ≥ 8 embryos per knockdown, with 50 or more embryos scored per knockdown (except †> 1000); ‡, embryos showed developmental defects. All data are reported as means ± SEM. Statistical significance versus the noninjected *p53^{e7/e7}* response: * $p < 0.05$; ** $p < 0.005$; *** $p < 0.0005$; ns (not significant), (two-tailed Student's t test).

(C) Fluorescent images of AO-labeled, live *p53* mutants injected with indicated MOs and representative of the phenotypes quantified in (B).
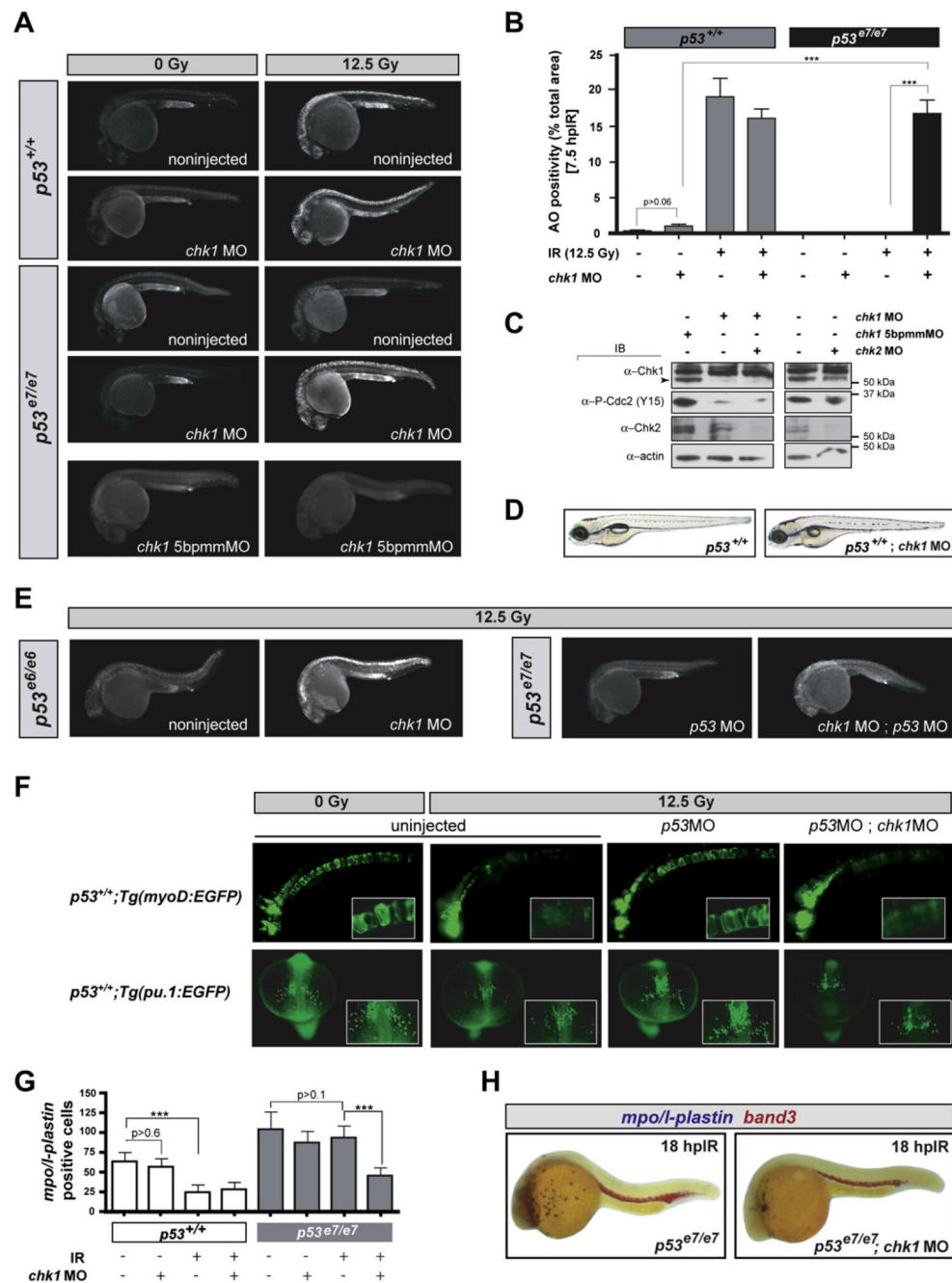
Figure 2. *chk1* Knockdown Radiosensitizes *p53* Mutants but Is Otherwise Compatible with Normal Zebrafish Development

(A) Fluorescent images of representative embryos of indicated genotypes +/− *chk1* MO after 0 or 12.5 Gy IR; 5bpmmMO (5 base pair mismatch MO).

(B) Quantified AO responses of indicated genotypes with or without IR (12.5 Gy) and *chk1* MO. Gray bars, *p53*^{+/+} background; black bars, *p53*[e7/e7] background. AO staining was quantified in ≥ 8 embryos per condition, with > 1000 embryos scored. All data are reported as means ± SEM *** p < 0.0001 (two-tailed Student's t test).

(C) Western blots comparing the levels of Chk1, Chk2, and phosphorylated Cdc2 (Tyr15) in protein lysates from 25.5 hpf embryos injected with the indicated MOs.

(D) Nonirradiated $p53^{+/+}$;$chk1^{MO}$ larva photographed live at 5 days postfertilization (dpf) show no apparent developmental defects but is slightly delayed (smaller swim bladder). Such larvae survived to adulthood.

(E) Fluorescent images of representative irradiated embryos of indicated genotypes. $p53^{e6}$ is the N168K mutation, corresponding to human residue 200. $p53MO$, MO against the $p53$ 5′ UTR.

(F) Fluorescent images of live transgenic embryos injected with the indicated MOs at the 1-cell stage and expressing EGFP in the notochord (top row, embryos photographed at 24 hpf) or in myeloid progenitors (bottom row, embryos photographed at 16.5 hpf). Tg $(myoD:EGFP)$ and $Tg(pu. 1:EGFP)$ embryos were treated with or without IR (12.5 Gy) at 18 hpf and 10 hpf, respectively. Insets, higher magnification views of GFP-expressing cells. Top row, lateral views, anterior to the left. Bottom row, dorsal views, anterior facing down.

(G) Quantification of myeloid cells in 28 hpf embryos generated as indicated (x axis) and processed as in (H). Gray bars, $p53^{+/+}$ background; black bars, $p53^{e7/e7}$ background. mpo/l-$plastin$ staining was quantified in $\geq$ 15 embryos per condition. Data are reported as means $\pm$ SD ** p < 0.001, *** p < 0.0001 (two-tailed Student's t test). Note that while the numbers of mpo/l-$plastin$-positive cells are reduced ~3-fold in IR-treated versus untreated $p53^{+/+}$ embryos; they are unchanged in treated versus untreated $p53^{e7/e7}$ embryos. Also note that $chk1$ knockdown induces an average 2-fold reduction in myeloid cell numbers in the $p53^{e7/e7}$ background after IR.

(H) Images of representative 28 hpf embryos of indicated genotypes processed for in situ hybridization of mpo and l-$plastin$ riboprobes (blue, differentiated granulocytes and monocytes) and $band 3$ (red, erythrocytes). Note the specific reduction in number of granulocytes/monocytes.
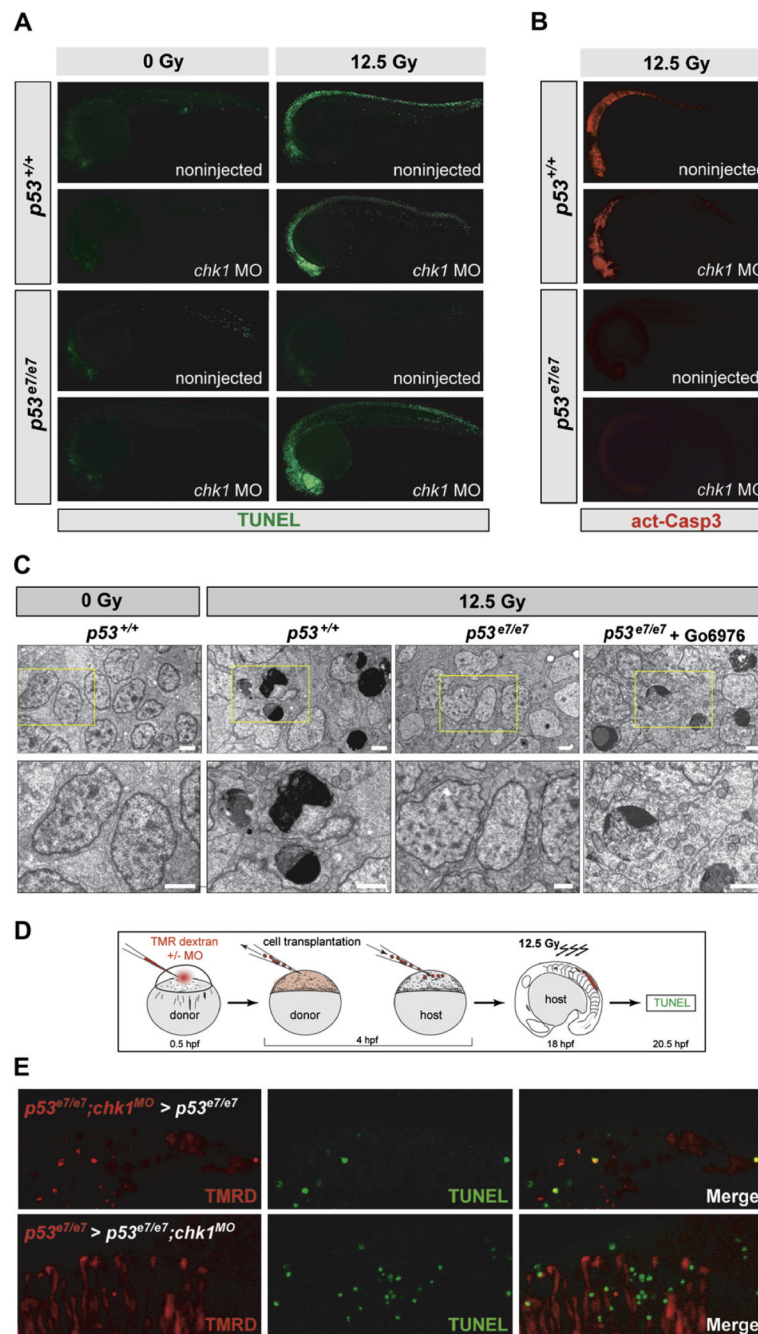
Figure 3. IR-induced p53-Independent Apoptosis after Chk1 Loss Occurs Cell Autonomously and Independently of Caspase-3

(A) Fluorescent images of 25 hpf embryos (anterior, left). TUNEL reactivity after IR (0 or 12.5 Gy) recapitulates live AO labeling (see Figure 2A).

(B) Embryos from the same experiment immunostained with an antiactivated-Caspase-3 antibody. Note the absence of immunoreactivity in the irradiated $p53^{e7/e7};chk1^{MO}$ embryo.

(C) Electron micrographs (sagittal sections) of the CNS in embryos of indicated genotypes after 0 or 12.5 Gy IR. Gö6976 is a specific Chk1 inhibitor (see Figure 5–Figure 7). Lower row, 2.5× closeups on the areas boxed in yellow in upper panels. Note multiple cells with stereotypical chromatin compaction/segregation in columns 2 and 4, as opposed to healthy

nuclei in columns 1 and 3. Organelles and plasma membrane are intact in the shown Chk1-inhibited irradiated *p53* mutant cell, as expected from an apoptotic (as opposed to necrotic) event. See Figure S2 for more details. Scale bar, 2 µM.

(D) Experimental procedure for the generation of the genetic chimeras shown in (E).

(E) 5-µm-thick confocal sections of spinal cords in irradiated chimeras. TMR Dextran (red) marks the donor cells. TUNEL shown in green. First row, cells from a $p53^{e7/e7}$ embryo that was injected with the *chk1* MO at the 1-cell stage ($p53^{e7/e7}$;$chk1^{MO}$ embryo) transplanted into a $p53^{e7/e7}$ host. Second row, $p53^{e7/e7}$ cells transplanted into a $p53^{e7/e7}$;$chk1^{MO}$ host.
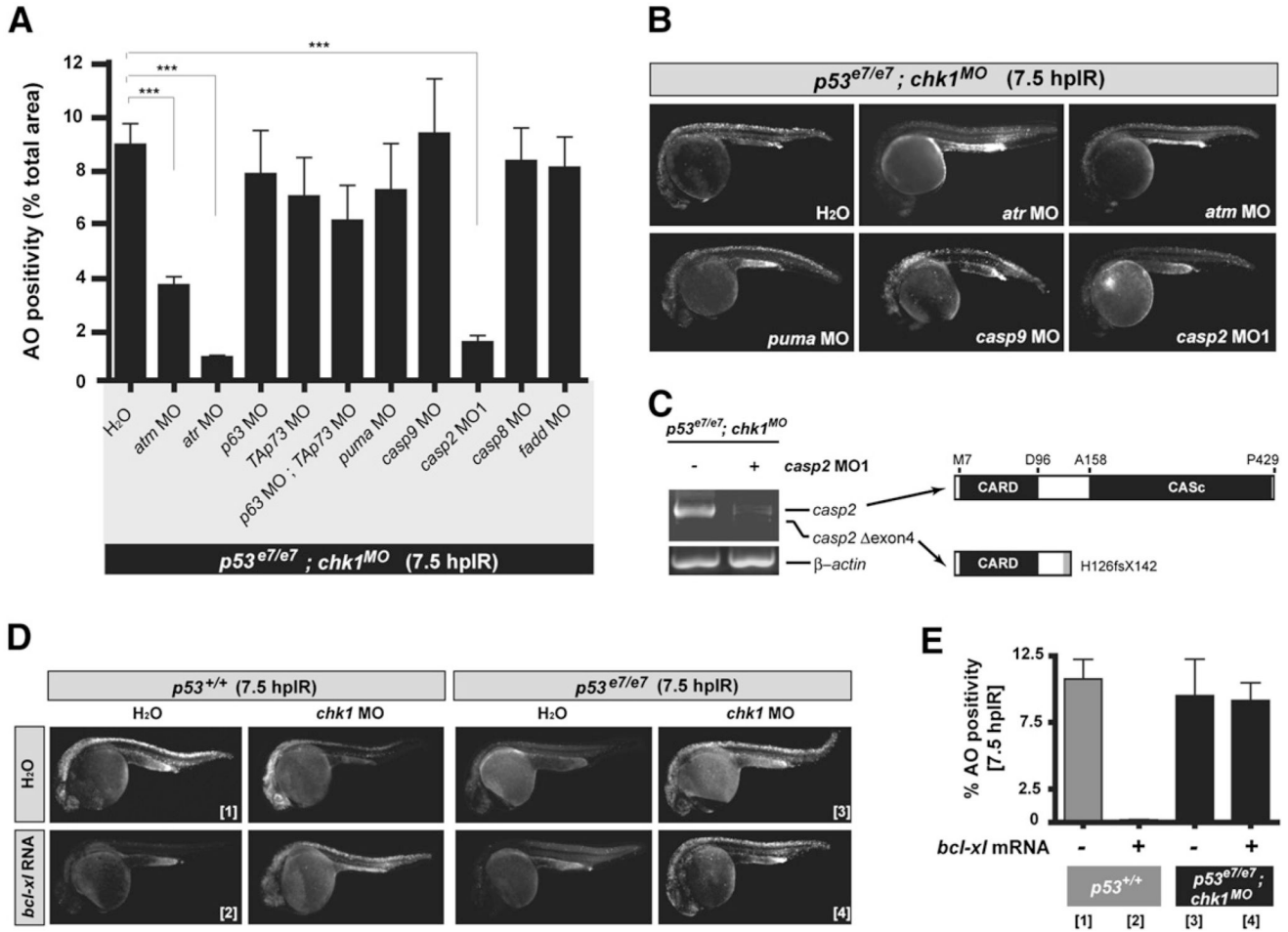
Figure 4. Genetic Dissection of the Zebrafish Chk1-Suppressed Apoptotic Pathway
(A) Quantified AO labeling in spinal cords of 12.5 Gy-exposed $p53^{e7/e7};chk1^{MO}$ embryos injected with H_2O (bar on the far left) or the indicated MOs (x axis). AO staining was quantified in ≥8 embryos per MO with a total of ≥100 embryos scored. All data are means ± SEM *** p < 0.0001 (two-tailed Student's t test).
(B) Fluorescent images of representative embryos from the experiments shown in (A).
(C) At left, RT-PCR of *casp2* transcripts from embryos either injected or not injected with *casp2* MO. At right, schematics of caspase-2 protein variants (top, wild-type protein; bottom, predicted protein translated from exon 4-deleted transcripts).
(D) Fluorescent images of embryos of the indicated genotypes with or without IR (12.5 Gy at 18 hpf), *chk1* MO, or *bcl-xl* mRNA. Numbers in brackets refer to the corresponding bars in (E).
(E) Quantified AO responses (n ≥ 8) for embryos of indicated genotypes +/− *bcl-xl* mRNA. Gray bars, $p53^{+/+}$ background; black bars, $p53^{e7/e7};chk1^{MO}$ background. Numbers in brackets refer to the representative-embryo images in (D). Data are means ± SEM.
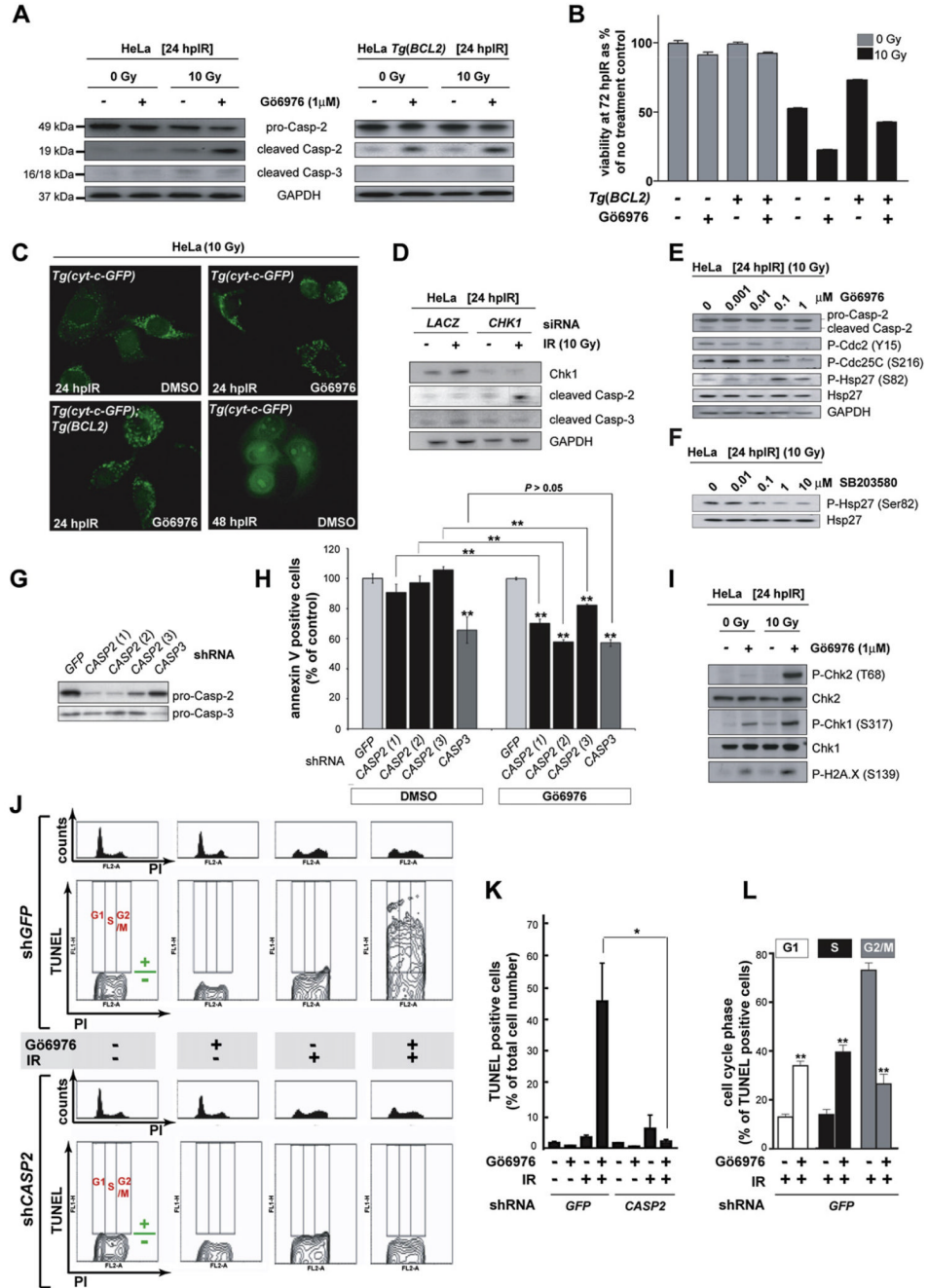
Figure 5. The Chk1-Suppressed Pathway Is Conserved in HeLa Cells
(A) Western blots comparing the levels of caspase-2 (pro and cleaved forms) and cleaved caspase-3 at 24 hpIR in lysates from HeLa cells carrying or not carrying a *BCL2* transgene (*Tg[BCL2]*) and treated with or without IR (10 Gy) or Chk1 inhibitor (Gö6976, 1 µM).
(B) Analysis of HeLa cell survival at 72 hpIR (0 Gy versus 10 Gy) in the presence or absence of Gö6976 and/or *BCL2*. Gö6976 radiosensitizes the cells ~2-fold regardless of the *BCL2* transgene (compare bars 5 and 6, and bars 7 and 8). Note that *BCL2* is functional (i.e., radioprotective) in these experiments (compare lanes 5 and 7). Data are means ± SEM.

(C) Fluorescent images of HeLa *Tg(Cyt-c-GFP)* cells with or without *Tg(BCL2)* or Gö6976 at 24 or 48 hpIR (10 Gy). Note the punctate GFP patterns in all 24 hpIR samples and the diffuse GFP pattern in the 48 hpIR sample.

(D) Levels of cleaved caspase-2 and caspase-3 at 24 hpIR (10 Gy) in HeLa cells transfected with *LACZ* or *CHK1* siRNAs at 72 hr before IR.

(E) Western blots comparing the activities of Chk1 (Cdc2 phosphorylation at Tyr15 and CDC25C phosphorylation at Ser216) and MK-2 (Hsp-27 phosphorylation at Ser82) following exposure to IR and increasing concentrations of Gö6976.

(F) MK-2 phosphorylates Hsp-27 in HeLa cells. Western blot of lysates from irradiated HeLa cells exposed to increasing concentrations of the p38MAPK specific inhibitor SB203580 (Reinhardt et al., 2007), showing a dose-dependent reduction in phosphorylated Hsp-27.

(G) Knockdown efficiencies of the indicated shRNAs as measured by western blots with anticaspase-2 and anticaspase-3 antibodies.

(H) Effects of *GFP, CASP2*, and *CASP3* shRNAs on apoptotic cell numbers at 48 hpIR as measured by AnnexinV (+) / PI (−) staining of HeLa cells treated with 10 Gy with or without Gö6976 (1 µM). For each shRNA, the average apoptotic cell number (given as % of *GFP* shRNA control) is shown. All data are means ± SD ** $p < 0.01$ (two-tailed Student's t test). Asterisks on top of bars refer to comparisons with *GFP* shRNA.

(I) Synergistic activation of ATM and ATR by Gö6976 and IR. Western blots comparing the activities of ATM (Chk2 phosphorylation at Thr68) and ATR (Chk1 phosphorylation at Ser317) after 0 or 10 Gy IR with or without Gö6976 (1 µM). Levels of DNA damage were detected with an antiphospho-H2A.X antibody. (J) Cell-cycle distribution of HeLa cells undergoing Chk1-suppressed apoptosis. HeLa cells harboring *GFP* or *CASP2* shRNAs and treated with or without 10 Gy IR with or without Gö6976 (1 µM), as indicated, were fixed at 48 hpIR and stained for TUNEL and PI. For each shRNA line, upper panels show PI-single histograms and lower panels show PI/TUNEL double-staining images. Cell-cycle phases and threshold for TUNEL positivity are indicated in red and green, respectively, in each no-treatment control images.

(K) Quantification of the TUNEL stains shown in (J). Data are means ± SEM * $p < 0.05$ (two-tailed Student's t test).

(L) Quantified data from experiment in (J) expressed as means ± SEM ** $p < 0.002$ (two-tailed Student's t test). White bars indicate cells dying in G1 phase. Black bars indicate cells dying in S phase. Grey bars, cells dying in G2 phase.
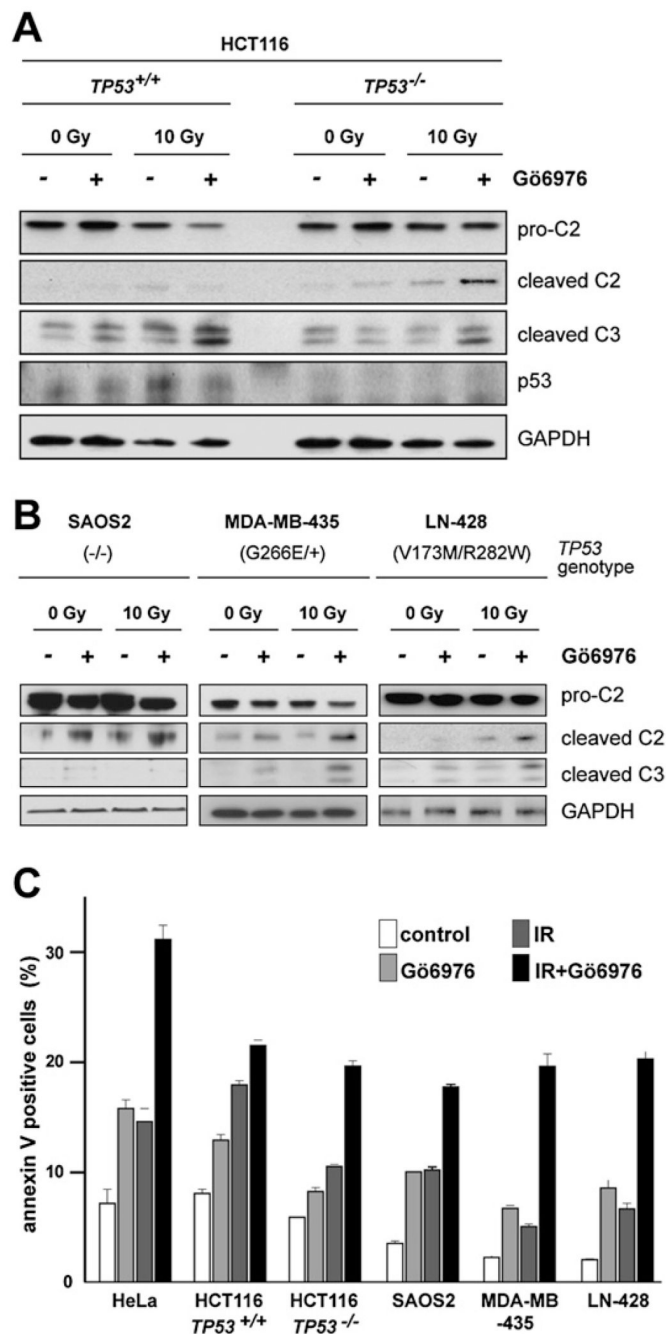
Figure 6. Influence of Genetic Background on Gö6976-Mediated Radiosensitization of Human Cancer Cells

(A) Western blots comparing the levels of caspase-2 (pro and cleaved forms) and cleaved caspase-3 in 24-hpIR lysates from $TP53^{+/+}$ and $TP53^{-/-}$ HCT116 cells that were treated with or without IR (10 Gy) or Gö6976 (1 µM).

(B) Analysis as in (A) of the SAOS2 (left), MDA-MB-435 (middle), and LN-428 (right) lines.

(C) Apoptotic cell numbers at 48 hpIR as measured by Annexin V (+) / PI (−) staining of the indicated cell lines treated with 0 or 10 Gy IR with or without Gö6976 (1 µM). Data are means ± SEM. See Figure S9 for a *CHK1* shRNA-mediated phenocopy of Gö6976 in $TP53^{-/-}$ HCT116 cells.
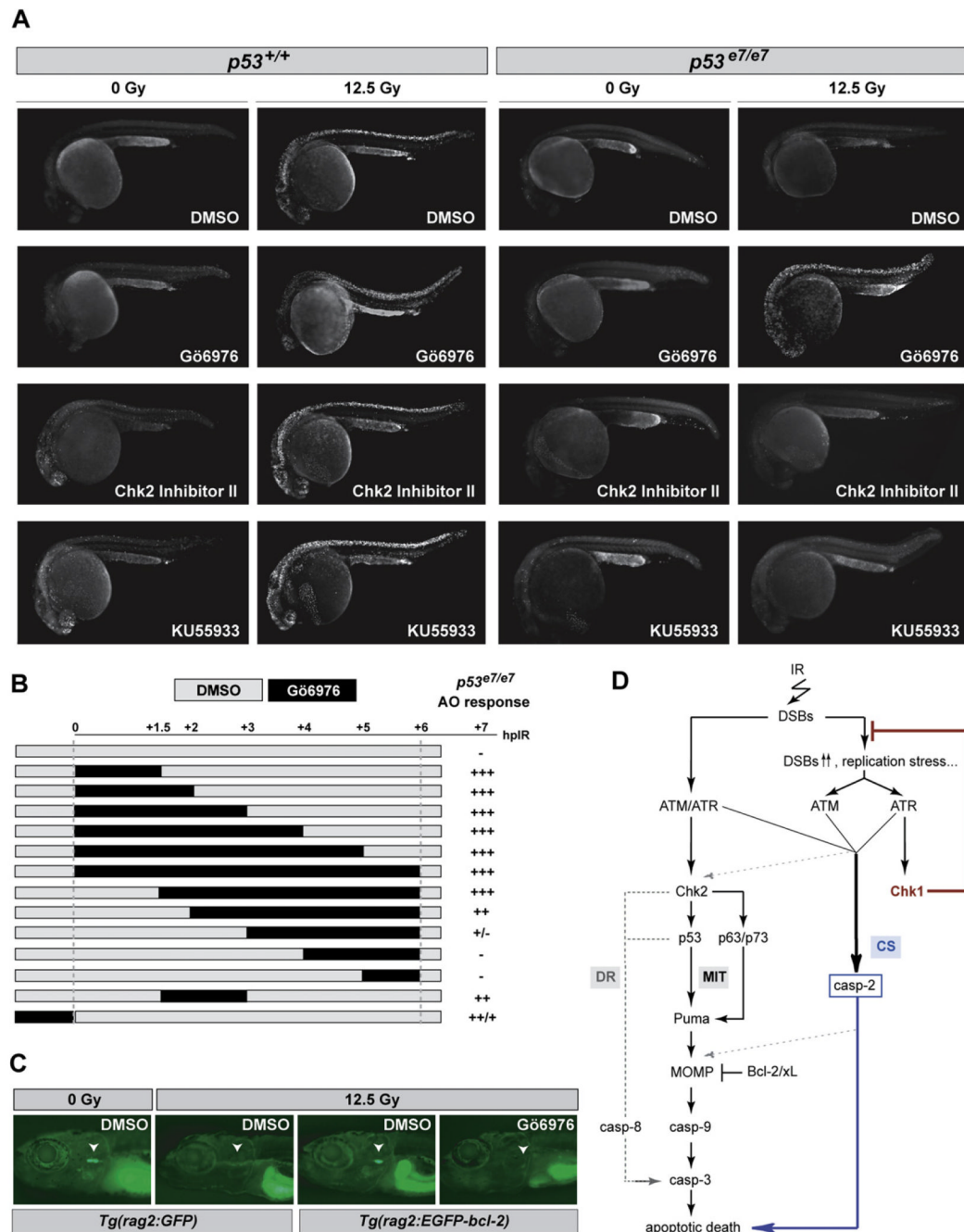
Figure 7. Effects of Gö6976 in Zebrafish In Vivo Models of p53 Loss and *bcl-2* Gain
(A) Fluorescent images of AO-labeled embryos of indicated genotypes photographed at 25.5 hpf. Embryos were exposed to 0 or 12.5 Gy IR and to the indicated drugs at 18 hpf. Gö6976, specific Chk1 inhibitor (1 µM). Chk2 Inhibitor II, specific Chk2 inhibitor (10 µM); KU55933, specific ATM inhibitor (10 µM). Note the range of toxicities in nonirradiated *p53*^{+/+} embryos treated with KU55933 or Chk2 Inhibitor II, with strong AO labeling preferentially localized in the brain and eyes (first column, third and fourth rows), as opposed to the Gö6976-treated embryo (first column, second row). Inversely, note the strong IR-induced AO labeling in the Gö6976-treated *p53* mutant (last column, second row), but the lack of staining in the mutants treated with KU55933 or Chk2 Inhibitor II (last column, third and fourth rows).

(B) Temporal requirement for Chk1 loss with respect to IR. *p53* mutant embryos were exposed to Gö6976 for the indicated times. AO staining was quantified on a scale from "−" to "+++"with "−" representing the *p53* mutant response and "+++" the response of sibling mutants treated with Gö6976 for 6 hr (~500-fold greater response).

(C) Fluorescent images of 9 dpf zebrafish larvae carrying the indicated transgene. Larvae were treated with 0 Gy or 15 Gy IR at 5 dpf and were exposed to Gö6976 (or DMSO as control) for a total of 5 days starting at 4 dpf. White arrowhead indicates the position of the thymus. Note the absence of detectable GFP in the Gö6976-treated *Tg(rag2:EGFP-bcl-2)* irradiated larva.

(D) Simplified model for the vertebrate apoptotic response to DNA damage, highlighting the p53-independent pathway normally blocked by IR-activated Chk1 (CS, for Chk1-suppressed pathway), which is distinct from the classical intrinsic (mitochondrial, MIT) and extrinsic (death-receptor, DR) pathways. See text for details.